International Journal of Pharmaceutics 366 (2009) 190–200

Contents lists available at ScienceDirect

International Journal of Pharmaceutics

journal homepage: www.elsevier.com/locate/ijpharm

Pharmaceutical nanotechnology

Microneedle mediated delivery of nanoparticles into human skin

Sion A. Coulman[a,*], Alexander Anstey[b], Chris Gateley[b], Anthony Morrissey[c], Peter McLoughlin[d], Chris Allender[a], James C. Birchall[a]

[a] Gene Delivery Research Group, Welsh School of Pharmacy, Cardiff University, Cardiff CF10 3NB, UK
[b] Gwent Healthcare NHS Trust, Royal Gwent Hospital, Cardiff Road, Newport, South Wales NP20 2UB, UK
[c] Biomedical Microsystems Team, Tyndall National Institute, Prospect Row, Cork, Ireland
[d] Waterford Institute of Technology, Cork Road, Waterford, Ireland

ARTICLE INFO

Article history:
Received 16 July 2008
Received in revised form 26 August 2008
Accepted 28 August 2008
Available online 4 September 2008

Keywords:
Microneedle
Nanoparticles
Transdermal
Skin
Skin permeation
Vaccination

ABSTRACT

The development of novel cutaneous delivery technologies that can produce micron-sized channels within the outermost skin layers has stimulated interest in the skin as an interface for localised and systemic delivery of macromolecular and nanoparticulate therapeutics. This investigation assesses the contribution of physicochemical factors to the rate and extent of nanoparticle delivery through microchannels created in a biological tissue, the skin, by novel delivery technologies such as the microneedle array.

The hydrodynamic diameter, zeta potential and surface morphology of a representative fluorescent nanoparticle formulation were characterised. Permeation studies using static Franz-type diffusion cells assessed (i) the diffusion of nanoparticle formulations through a model membrane containing uniform cylindrical microchannels of variable diameter and (ii) nanoparticle penetration across microneedle treated human skin.

Wet-etch microneedle array devices can be used to significantly enhance the intra/transdermal delivery of nanoparticle formulations. However the physicochemical factors, microchannel size and particle surface charge, have a significant influence on the permeation and subsequent distribution of a nanoparticle formulation within the skin. Further work is required to understand the behaviour of nanoparticle formulations within the biological environment and their interaction with the skin layers following disruption of the skin barrier with novel delivery devices such as the microneedle array.

1. Introduction

Significant developments in molecular biology and expansion of the biotechnology industry has resulted in the advancement of therapeutics from low molecular weight compounds to a diverse range of macromolecular agents including peptides, proteins and nucleic acids. This has been accompanied by developments in pharmaceutical formulation technologies and the evolution of numerous nanoparticle carrier systems that aim to improve the cellular and sub-cellular targeting, stability and toxicity profiles of the active agents. However the therapeutic usefulness of novel nanoparticle formulations is intrinsically linked to effective delivery of the formulation to its target tissue.

The skin is a lucrative interface for the delivery of therapeutics for systemic or local effects. Conversely, the inherent function of the outermost layer of this tissue, the stratum corneum (SC), is to provide a barrier to the ingress of exogenous material and the invasion of micro-organisms (Elias, 1983, 2005; Scheulplein and Blank, 1971). Investigations in recent years have assessed the penetration of metal (Baroli et al., 2007), lipid-based (Kuntsche et al., 2008; Papazoglou et al., 2008; Sanna et al., 2007), polymeric (Alvarez-Roman et al., 2004; Kohli and Alpar, 2004; Sheiheta et al., 2008) and other (Lademann et al., 1999; Zhang and Monteiro-Riviere, 2008; Zhang et al., 2008) nanoparticles across the outer skin layers in an attempt to determine (i) the potential therapeutic benefits of nanoparticle delivery systems (Salata, 2004) and (ii) the possible health risks (Hoet et al., 2004) associated with the penetration of nanoparticle material through the skin barrier. These studies indicate that topically applied nanoparticles are primarily restricted to the uppermost stratum corneum layers (Kuntsche et al., 2008; Lademann et al., 1999; Zhang et al., 2008) and the hair follicles (Alvarez-Roman et al., 2004; Lademann et al., 2007; Toll et al., 2003). However, it should be noted that the penetrative abilities of nanoparticles through human skin are complex and are determined by the material properties of the nanoparticle, the size of individual particles, their shape and other physicochemical factors.

* Corresponding author. Tel.: +44 2920874538; fax: +44 2920874149.
E-mail address: coulmansa@cardiff.ac.uk (S.A. Coulman).

0378-5173/$ – see front matter © 2008 Elsevier B.V. All rights reserved.
doi:10.1016/j.ijpharm.2008.08.040

Traditionally, transdermal delivery has been restricted to elegant formulation strategies to enhance the delivery of potent lipophilic molecules possessing a molecular weight of less than 500 Da (Bos and Meinardi, 2000; Mitragotri, 2004). However, in the last decade a number of novel delivery devices have been engineered to enhance the delivery of therapeutics across the skin barrier (Barry, 2001, 2002; Chiarello, 2004; Coulman et al., 2006a; Cross and Roberts, 2004; Gadiraju et al., 2007; Lee et al., 2008; Liu et al., 2008; Prausnitz et al., 2004; Schuetz et al., 2005; Ting et al., 2004). These include 'physical' delivery methods, e.g. microscission, thermal poration, radio-frequency ablation and microneedle application which create micron-sized portals within the skin. Temporary perforation of the SC therefore reduces the physical barrier of the skin and may permit intra/transdermal delivery of a greater number of therapeutic compounds. In recent years the potential applicability of these devices to the vaccination process has been recognised, initiated in part by a rejuvenated interest in the intradermal route of vaccination (Frerichs et al., 2008; Glenn and Kenney, 2006; Hirschberg et al., 2008; Kenney et al., 2004; La Montagne and Fauci, 2004). Novel delivery devices such as the microneedle array are therefore being investigated as simple and minimally invasive methods to deliver both existing and novel vaccine candidates (Giudice and Campbell, 2006; Mikszta et al., 2002, 2005; Prausnitz, 2004; Widera et al., 2006), including nanoparticles (Combadiere and Mahe, 2008; Lawson et al., 2007; Manolova et al., 2008), to human subjects.

Although it is intuitive to assume that microchannels created through the SC will readily facilitate the intra-epidermal penetration of nanoparticle formulations, the movement of a charged colloidal system through micron-sized conduits within the skin tissue is a complex and poorly understood process that has received limited investigation (Campbell, 2006; Florence, 2007; Nasseri and Florence, 2005; Ruenraroengsak and Florence, 2005). Increased understanding of nanoparticle dynamics following their topical or intradermal deposition by novel drug delivery devices will inform the development of both the device and the pharmaceutical formulation, thus facilitating optimisation of the delivery system. Predicted impediments to successful intradermal delivery of macromolecular and nanoparticle formulations include (i) non-covalent interaction with the skin surface and other components of the tissue, (ii) formulation instability/flocculation, (iii) steric hindrances and (iv) degradation of the therapeutic/formulation within the biological environment.

The aims of this study are to investigate the influence of surface charge and pore size on the penetration of a colloidal formulation through well-defined microchannels and to facilitate delivery of a fluorescent polymeric nanoparticle formulation through microneedle treated human skin. These studies will contribute to the progressive development of formulation strategies for minimally invasive technologies, including the microneedle array, as methods for intra/transdermal delivery of nanoparticle/macromolecular therapeutics.

2. Materials and methods

2.1. Materials

All reagents were obtained from Fisher (Loughborough, UK) unless stated otherwise and were of analytical grade.

Fluorescent yellow/green polystyrene amine-modified nanospheres (L-1280), propranolol hydrochloride, chloroform and Greiner® 96-well polypropylene plates were obtained from Sigma–Aldrich Chemical Company (Poole, UK).

All histology materials including optimal cutting temperature (OCT) embedding media and Histobond® adhesive microscope slides were obtained from RA Lamb Limited (Eastbourne, UK) or in the case of toluidine blue, Harris' haematoxylin, Gurrs' eosin aqueous solution 1%, Histomount® and xylene (low sulphur) from Lab 3 (Bristol, UK).

The microneedle arrays used in this study were supplied by The Tyndall National Institute, Cork, Ireland. Pyramidal microneedles were fabricated using wet-etching in potassium hydroxide and subsequent coating with a 0.3 μm layer of platinum (Birchall et al., 2005; Coulman et al., 2006b; Haq et al., 2008; Pearton et al., 2008; Wilke et al., 2005).

2.2. Fluorescent nanoparticle characterisation

Fluorescent nanospheres possess a surface bound fluorophore possessing excitation and emission values of 470 and 505 nm, respectively. These values were confirmed by excitation and emission scans using a U-300 spectrophotometer (Hitachi, Tokyo, Japan) with a slit width of 2 μm and a scan range of 200–800 nm. The proprietary nanosphere preparation contains latex nanospheres, surfactant and inorganic salts. These were diluted before measurement using deionised water.

2.2.1. Transmission electron microscopy (TEM)

A pioloform-coated 200-mesh nickel grid was fixed between the tips of a metal forceps and 15 μl of the nanoparticle formulation was applied to the grid. After 3 min, excess formulation was removed and the grid was then positioned on the surface of a filtered 2% aqueous uranyl acetate drop for 30 s. Excess stain was then 'wicked' from the grid, which was subsequently rinsed in deionised water before visualisation using a Philips 208 Transmission Electron Microscope (Philips, Eindhoven, The Netherlands).

2.2.2. Photon correlation spectroscopy (PCS) size analysis

Measurements were performed using the Coulter N_4 Plus PCS instrument (Coulter electronics, Luton, UK). Unimodal analysis provided a mean particle size and standard deviation (S.D.) for a monodisperse suspension. However for more complex distributions a size distribution processor (SDP) analysis was used. Fluorescent nanosphere samples were prepared by dilution with filtered deionised water in a clear-sided disposable cuvette.

2.2.3. Zeta potential

The zeta potential was determined for the nanoparticle formulation using a pre-calibrated Malvern 2000 Zetasizer (Malvern Instruments, Malvern, UK). Briefly, the nanoparticle formulation was diluted with deionised water and injected into a flow through cell, allowed to equilibrate for 30 s and then analysed repeatedly ($N = 5$) before removal. The effect of progressive changes in pH on the zeta potential of the nanosphere suspension was determined using a multi-purpose titrator (Malvern Instruments, Malvern, UK) with the pH adjusted progressively using 0.1 M hydrochloric acid and 0.1 M sodium hydroxide.

2.3. Predictive nanoparticle diffusion studies using Isopore® membranes

Isopore® membranes were mounted between the donor and receptor chambers of static Franz type diffusion cells of known receptor volume (mean volume 3.58 ml) and diffusional area. Each membrane was 27 mm in diameter and possessed a pore size of 100 nm, 1.2 or 10 μm. The receptor compartment of each cell was filled with degassed deionised water that was adjusted to a specific pH value (pH 3 or pH 7.4) using sodium hydroxide (1 M) or

hydrochloric acid (1 M), and was maintained at 37 °C in a water bath. The receptor phase, was continuously agitated and the receptor sampling arm of diffusion cells were covered with a foil cap. Cells were allowed to equilibrate for at least 30 min before application of 500 μl of a nanoparticle formulation that consisted of the proprietary preparation diluted with de-ionised water. This formulation contained 10.9×10^6 nanoparticles. Following application the donor chamber was occluded. The pH of each of the applied fluorescent nanosphere formulations was adjusted to complement that of the receptor phase.

Samples (200 μl) were removed from the receptor arm at regular intervals over a period of 12 h and replaced with an equal volume of receptor phase (37 °C). A sample was also removed from the donor phase of each cell at the conclusion of the experiment. Samples were stored in a Greiner® black polypropylene 96-well plate and analysed using a Fluostar® fluorometer (BMG Laboratories, Offenburg, Germany). Fluorescence values were converted to concentrations of fluorescent beads and the percentage of the applied formulation in each of the compartments (donor and receptor) was determined at the conclusion of the experiment. The sum of these values was then used to calculate the amount of the applied formulation that was theoretically bound to the membrane and/or diffusion cell surface.

Following removal of the final sample, diffusion cells were dismantled and the pH of receptor phases was determined. Isopore® membranes were retained for microscopic evaluation using an Olympus IX-50 fluorescence microscope (Olympus Optical, London, UK) and were subsequently mounted on an aluminium stub, gold sputter coated (EM Scope, Kent, UK) and assessed by a Philips XL-20 Scanning Electron Microscope (Philips, Eindhoven, The Netherlands).

2.4. Scanning electron microscopy (SEM) of silicon microneedle arrays

Silicon microneedle structures can vary within and between microfabrication runs and therefore the shape and morphology of each device was inspected prior to experimentation. It was not necessary to sputter coat the sample prior to SEM and so devices were simply mounted upon an aluminium stub and assessed using a Philips XL-20 Scanning Electron Microscope (Philips, Eindhoven, The Netherlands).

2.5. Propranolol diffusion through microneedle treated human epidermal membranes

Human breast skin was obtained from mastectomy or breast reduction procedures with full ethical committee approval and informed patient consent. In these studies, human skin from a 67-year-old female donor was removed from storage at −20 °C and allowed to equilibrate over 1 h. Subcutaneous fat was removed by blunt dissection and the epidermal membrane was isolated by heat separation (Christophers and Kligman, 1963) and collected on aluminium foil. The epidermal sheet was then replaced on the dermal tissue from which it was removed. A microneedle device (pointed tipped, wet-etch) with an area of 1 cm^2 was mounted on a steel rod and then applied to the epidermal sheet, by hand, using a force of approximately 2 kg/cm^2. This same area of tissue was treated a further four times, with an interval of 5 s between applications. Therefore a single area of the epidermal sheet was treated a total of five times with the microneedle device. This treatment process was repeated to produce a total of six microneedle treated areas ($N = 6$). Each treatment area, including a surrounding perimeter of untreated membrane, was then carefully isolated from the epidermal sheet (total area 2.5 cm^2) to ensure that the central treated region of the membrane was not damaged in the process. Four untreated areas of membrane were also isolated. Individual membranes were then mounted in Franz-type diffusion cells (Section 2.3). Finally, 0.5 ml of a 0.5 mg/ml (1.7 mM) propranolol hydrochloride formulation, containing the drug dissolved in de-ionised water, was applied to the microneedle treated ($N = 4$) and untreated ($N = 4$) epidermal membranes. Deionised water was applied to the remaining two microneedle treated epidermal membranes as a control ($N = 2$).

Samples (200 μl) were removed from the receptor phase over a 24 h period and subsequently, upon conclusion of the experiment, from the donor phase (Section 2.3). All samples were analysed by fluorescence spectrophotometry (BMG laboratories, Offenburg, Germany), with excitation and emission filters set at 280 and 330 nm, respectively. This assay was sensitive to levels of at least 0.001 mg/ml of propranolol hydrochloride, therefore enabling it to detect up to 0.02% of the applied formulation.

2.6. Nanoparticle diffusion through microneedle treated human epidermal membrane

Human epidermal membranes were isolated from a 67-year-old donor and either treated with a microneedle on five consecutive occasions ($N = 8$), or were left untreated ($N = 2$), before being mounted in static Franz-type diffusion cells as previously described (Section 2.5). Additionally, two 1 cm^2 areas of epidermal membrane were treated ten times by manual vertical application of a 26 G hypodermic needle ($N = 2$), ensuring that the needle penetrated through the entire width of the tissue. These were also mounted in Franz-type diffusion cells, in order to provide a positive control. The diffusion of the fluorescent nanosphere formulation through microneedle treated and untreated epidermal membranes was evaluated following application of 200 μl of nanosphere formulation to the donor phase (containing 5.44×10^8 nanoparticles). This topical formulation contained a greater quantity of nanospheres than the previous experiment (Section 2.3). This was necessitated by the heightened levels of background fluorescence that were measured upon employment of the human epidermal membrane in the experimental set-up and hence the reduced assay sensitivity. Deionised water was applied to the donor phase of microneedle treated membranes to serve as a negative control ($N = 4$).

Receptor phase samples were removed from the sampling arm at specific time-points over the duration of the experiment (72 h) and subsequently analysed by fluorescence spectrophotometry, as previously detailed (Section 2.3).

Upon conclusion of diffusive studies, the Franz-type cells were dismantled and the human epidermal membrane was retained for microscopic inspection. The tissue was fixed (2.5% glutaraldehyde) and subsequently dehydrated (ethanol gradient 70%, 90%, 100%). A Bal-Tec CPD030 Critical Pont Drier (Bal-Tec, Balzers, Lichenstein) was used to complete dehydration of the specimen, which was finally mounted on an aluminium stub and gold sputter coated in preparation for SEM analysis.

3. Results and discussion

3.1. Fluorescent nanoparticle characterisation

In order to investigate the influence of physicochemical parameters on nanoparticle delivery, great care was taken not only to develop a model system with biological relevance but also to impose reasonable limits on how resulting data would be extrapolated to biological systems. A series of predictive studies, using a synthetic membrane (Section 3.2), were designed to determine

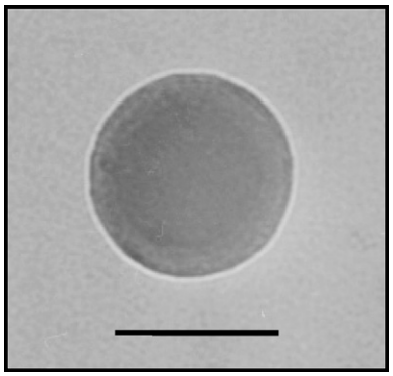

Fig. 1. A TEM image of a fluorescent nanosphere. Scale bar = 100 nm.

the importance of particle size and surface charge (zeta potential) on the permeation of nanoparticles through microchannels created within the skin surface by novel transdermal delivery devices. Fluorescent nanospheres, used previously as model nanoparticles (Alvarez-Roman et al., 2004; Kohli and Alpar, 2004), were selected as a simple, well-defined, detectable and quantifiable representation of a nanoparticle delivery system.

TEM images indicated that the fluorescent spherical nanoparticles possess a diameter of between 100 and 150 nm (Fig. 1). This was confirmed by PCS analysis (mean nanoparticle diameter 138 ± 25.1 nm; $N = 5$). It might be anticipated that microconduits created in the skin surface by novel transdermal delivery devices must be greater than this measured nanoparticle diameter to ensure successful transdermal permeation.

Zeta potential provides a measure of the charge that a colloidal particle adopts within a defined aqueous media. The zeta potential of nanoparticle formulations was measured at discriminate pH values between 2 and 12 (Fig. 2). This illustrated the direct influence of pH on the zeta potential of a colloidal particle and from this data an isoelectric point (the pH value of a colloidal formulation at which the zeta potential becomes 0 mV) of approximately pH 5 was calculated (Fig. 2). In simple terms, an isoelectric value of pH 5 means that within this particular aqueous environment hydrogen ions are required to neutralise what must be a dominant negative charge on the surface of the nanoparticle. Therefore although the nanoparticles have been functionalized to include reactive amine groups, it is negatively charged sulphate groups (created on the surface of the nanoparticle during the polymerization process) which contribute more significantly to the surface potential of the particle. The ability to reverse the zeta potential of nanoparticles, by adjustment of pH, was utilised to investigate the influence of a particles surface potential on its permeation through microconduits.

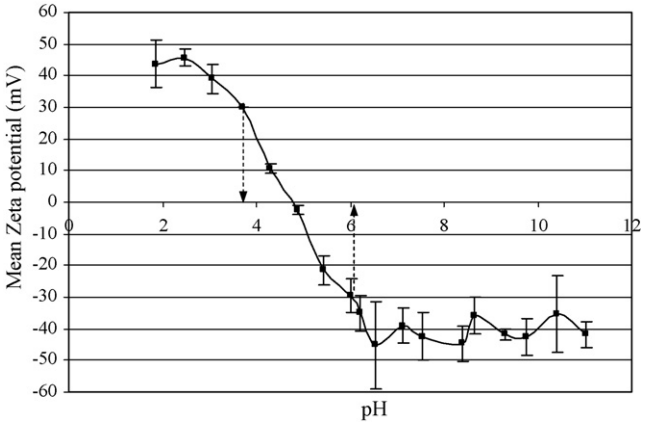

Fig. 2. The zeta potential of an aqueous suspension of nanospheres with pH values adjusted between 2 and 12. Dashed arrows indicate the pH range between which the zeta potential of the nanoparticle formulation falls between +30 and −30 mV. Mean ± S.D. ($N = 3$).

Electrostatic repulsion between particles is often used as a method to maintain the stability of an aqueous colloidal suspension. Therefore in the design of such formulations the pH of the surrounding medium must be controlled to ensure that particles do not adopt zeta potential values between −30 and +30 mV (colloidal suspensions within this range are considered unstable (Sugrue, 1992)). In this investigation, adjustment of the nanoparticle formulation pH to between 3.5 and 6 induced the progressive aggregation of nanoparticles (data not shown) due to the reduction in repulsive forces between particles (Fig. 2). Effective control of the formulation pH when delivering a colloidal system through conduits created by microneedles will therefore be critical to prevent particle aggregation and subsequent entrapment of large aggregates on the skin surface. Such factors should be considered when using novel transdermal delivery devices to promote delivery of colloidal formulations through microchannels that have been created in the skin barrier.

3.2. Predictive nanoparticle diffusion studies using Isopore® membranes

The presence of uniform, well-characterised micropores was a principle selection criterion for the synthetic membranes used to study nanoparticle movement through microchannels. Isopore® polycarbonate track-etched membranes possess cylindrical microchannels of measurable diameter and length (Apel, 2001; Brendler et al., 1995; Diez et al., 1989) and negative surface potentials (Brendler et al., 1995), attributable to carboxylic acid groups that are created on the pore surface during membrane manufacture (Huismann et al., 2000; Keesom et al., 1988). The magnitude of this negative surface potential is relatively low, much like the skin surface, a membrane with a net negative charge which is imparted by the dominance of negatively charged amino acids (Burnette and Ongpipattanakul, 1987) and the presence of electron dense desmosomes (Wertz and Van Den Bergh, 1998). However, both the Isopore® membrane and the skin barrier retain a general hydrophobic character (Keesom et al., 1988).

Isopore® membranes were considered to be a gross representation of human skin containing microchannels, such as those created by a skin puncturing device, e.g. microneedle array device. Early studies by Prausnitz and co-workers used silicon microneedles, possessing sharp tips and a length of 150 μm, to produce 1 μm diameter conduits in the skin surface (Henry et al., 1998). However subsequent studies have demonstrated that microchannels with significantly greater diameters, e.g. 50–100 μm, can be created (Coulman et al., 2006b). Isopore® membranes possessing microchannel diameters of 1.2 μm (based on the findings of Henry and co-workers (Henry et al., 1998)), 10 μm (to determine the influence of increased pore size on diffusion) and 100 nm diameter (as a size restrictive control) were therefore selected for nanoparticle diffusion studies.

Experiments were also designed to determine the influence of nanoparticle surface potential on permeation. A pH of 7.4 was selected to represent physiological pH and to ensure that fluorescent nanospheres possessed a negative zeta potential (−40 mV) whilst at pH 3 the surface potential of fluorescent nanospheres was reversed, i.e. the zeta potential was approximately +40 mV (Fig. 2). Traditional buffer salts were not used to control pH due to their unpredictable effects on the measurement of zeta potential. However the pH of the receptor phase in all Franz-type diffusion cells

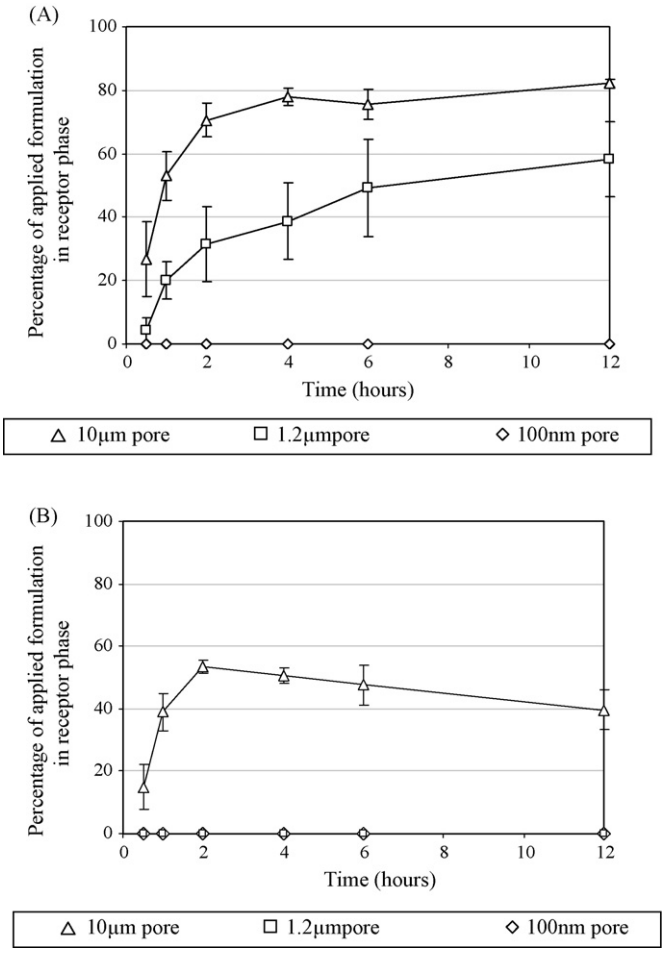

Fig. 3. Diffusion profiles illustrating the percentage of the applied nanoparticle formulation detected within the receptor phase of Franz-type diffusion cells over a period of 12 h. Isopore® membranes possessing three different pore sizes were used and the nanosphere formulation and receptor phases were maintained at either ~pH 7.4 or ~pH 3. (A) pH 7.4 mean ± S.D. ($N = 4$); (B) pH 3 mean ± S.D. ($N = 4$).

was measured both before and after each experiment and indicated that the desired pH was maintained for the duration of the experiment (data not shown).

At pH 7.4, where both the nanospheres and the membrane surface possess negative zeta potentials, diffusion through 10 μm pores occurred rapidly (Fig. 3A). After 4 h almost 80% of the applied formulation was detected in the receptor phase. At this stage the concentration of nanoparticles is approaching equivalence across the membrane, suggesting that permeation in this model is a simple diffusive process and that equilibrium can be reached in a relatively short period of time. Such rapid diffusion, facilitated by the significant difference between the microchannel and nanoparticle diameters, is particularly important for the cutaneous delivery of novel nanoparticle/macromolecular therapeutic formulations, particularly those from the biotechnology industry. Extended residency of these formulations within the superficial skin layers may result in interaction with extracellular tissue components, enzymatic degradation, immunological inactivation or another time-dependent process that impedes effective delivery of the therapeutic to the target region (Barry et al., 1999; Ruponen et al., 2003).

The rate of diffusion through 1.2 μm pores was significantly reduced, resulting in a failure to reach equilibrium between the donor and receptor phases and penetration of only 60% of the applied formulation during the 12 h experimental period (Fig. 3A). It is likely that the reduction in the rate of diffusion was directly attributable to the decrease in pore size, although a variation in charge density within the pores may have also contributed. The charge density on the internal surface of individual microchannels is determined by the surface area and the number of exposed carboxylic acid groups (during manufacture, longer etching times are used to create larger pore sizes and this exposes a greater number of carboxylic acid groups). Failure to detect nanoparticles in the receptor compartment of cells containing membranes with 100 nm pores suggested a simple size exclusion event and acted as a negative control to confirm the validity of the analytical method (Fig. 3A).

Reversal of the zeta potential, induced by reduction of the formulation pH to 3, resulted in considerable changes to the permeation characteristics of the nanoparticle formulation (Fig. 3B). At 2 h after topical application to the 10 μm pore membrane only 50% of the formulation was detected in the receptor phase (Fig. 3B), whereas at pH 7.4 over 70% of the applied formulation had permeated (Fig. 3A). Further, at pH 3 trans-membrane permeation appeared to halt at the 2 h time point and subsequent to this fluorescence levels in the receptor phase appeared to diminish (Fig. 3B). The modification in diffusion characteristics, induced by the reduction in pH, was even more dramatic for the 1.2 μm pores (Fig. 3B). Under these conditions any nanoparticle migration was below the detection limit of the analytical method.

This gross change in permeation characteristics was attributed to reversal of the nanoparticles surface potential and its resultant electrostatic interaction with the membrane surface. For 10 μm pores, the high pore diameter: particle diameter ratio (1 0 0) was insufficient to prevent particle migration. However permeation was significantly retarded and appeared to stop after the 2 h time-point, possibly due to the blockage of pores (Fig. 3B). The subsequent reduction in receptor phase concentrations may be explained by electrostatic interaction of the positively charged nanoparticles with the underside of the membrane or the walls of the diffusion cell. For 1.2 μm pores, the significant impediment to nanoparticle permeation was attributed to immediate adsorption of nanoparticles to the membrane surface and rapid accumulation, resulting in occlusion of microchannels (Fig. 3B).

Mass balance data aimed to calculate the percentage of the applied formulation that was bound to the membrane and/or the surface of the diffusion cell (Table 1). At the conclusion of experiments conducted at pH 7.4 more than 90% of the applied nanoparticle formulation was present in either the donor or receptor phase of the Franz-type diffusion cell. However for experiments conducted at pH 3 up to 56% of the applied formulation was not detected in either the donor or receptor phases and thus was predicted to be bound to the membrane and/or the surface of the diffusion cell (Table 1). Interestingly, a significantly greater percentage of the formulation was determined to be membrane bound when the pores exceeded 100 nm. This may be explained by the ability of nanoparticle to penetrate into the 1.2 and 10 μm membrane pores and to subsequently interact with the underside of the membrane, thus increasing the surface area available for nanoparticle adsorption. Fluorescent images of the membranes, recovered at the conclusion of the experiment, confirmed a marked difference in the interaction of nanoparticles with the membrane surface at the two studied pH values (Fig. 4). Significantly greater levels of observable fluorescence on the membranes isolated from experiments conducted at pH 3 also suggests that there is greater nanoparticle interaction with the membrane under these conditions. Further, SEM images also depict a significantly greater density of nanoparticles on those membranes maintained at pH 3 (Fig. 5). Together these results therefore support the hypothesis

Table 1
A summary of the distribution of the fluorescent nanosphere within the Franz-type diffusion cell at the conclusion of diffusion experiments

Latex nanosphere	Zeta potential (mV)	Percentage in DONOR phase at 12 h			Percentage in RECEPTOR phase at 12 h			Calculated BOUND percentage		
		100 nm	1.2 μm	10 μm	100 nm	1.2 μm	10 μm	100 nm	1.2 μm	10 μm
pH ~3	39.1 ± 4.6	70.1 ± 8.4	50.5 ± 7.6	4.1 ± 1.5	0 ± 0	0.1 ± 0	39.6 ± 6.4	29.9 ± 8.4	49.5 ± 7.7	56.3 ± 7.5
pH ~7.4	−39.0 ± 5.7	91.2 ± 7.4	37.9 ± 16.2	8.9 ± 0.2	0 ± 0	58.3 ± 11.7	82.3 ± 1.2	8.8 ± 7.4	3.8 ± 4.6	8.8 ± 1.3

Values are expressed as mean ± S.D. ($N = 4$).

that reversal of the nanoparticles zeta potential, from negative to positive, encourages electrostatic interaction with the membrane surface.

The permeation of a nanoparticle formulation through a microporous membrane is therefore dictated, at least in part, by the surface potential of nanoparticles and the magnitude and charge of the microchannels that traverse the membrane structure. Therefore although marked differences between synthetic membranes and the skin tissue are acknowledged, such physicochemical parameters must be considered during development of nanoparticle

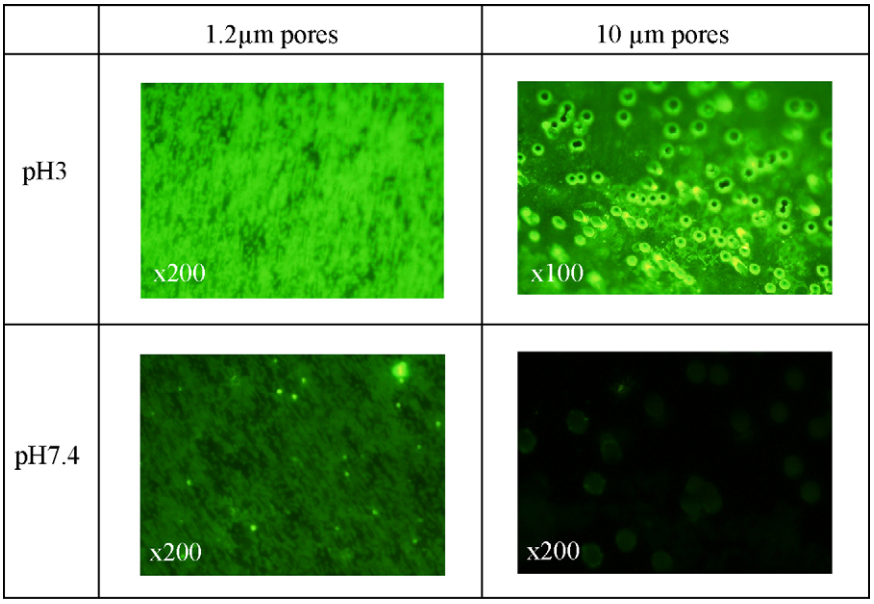

Fig. 4. Fluorescent images of Isopore® membranes isolated from Franz-type diffusion cells subsequent to diffusion experiments conducted at both pH 3 and pH 7.4. Pore size and pH are indicated within the table structure and magnifications are detailed as inserts.

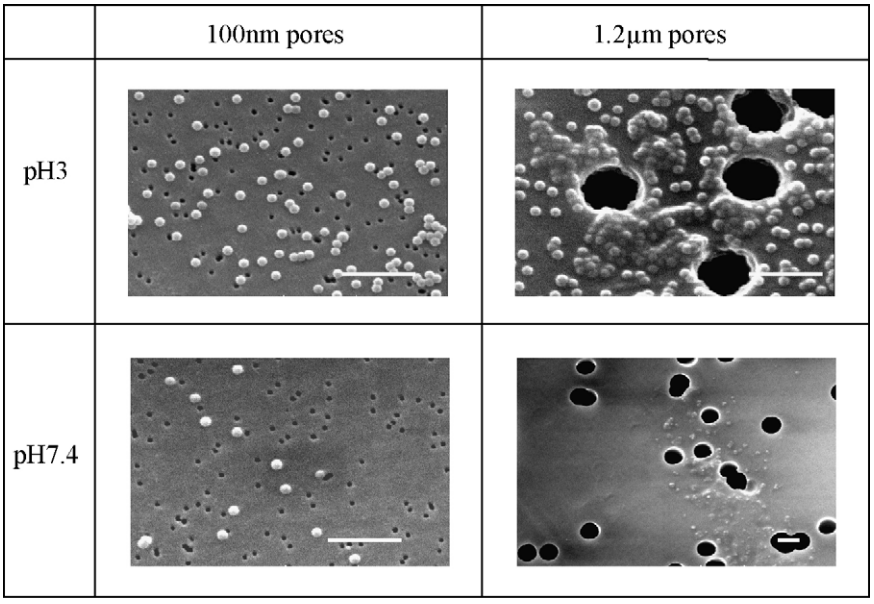

Fig. 5. SEM images of Isopore® membranes isolated from Franz-type diffusion cells subsequent to diffusion experiments conducted at both pH 3 and pH 7.4. Pore size and pH are indicated within the table structure. Scale bar = 1 μm.

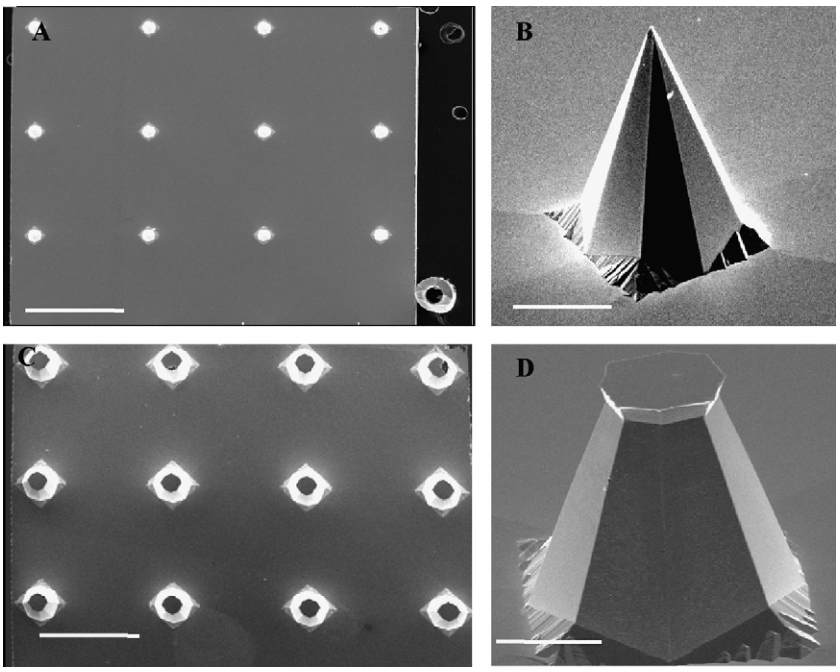

Fig. 6. SEM images of solid silicon pointed (A and B) and frustum (C and D) tipped microneedles, created by wet-etch engineering methods. (A and C) scale bar = 1000 μm; (B and D) scale bar = 100 μm.

formulations that are to be delivered across the skin using such novel delivery devices such as the microneedle array.

3.3. Scanning electron microscopy of silicon microneedle arrays

Silicon microneedle array devices have been extensively studied as a means of creating trans-SC microconduits in order to increase the permeability of the skin barrier to low molecular weight compounds and macromolecules (Birchall et al., 2005; Coulman et al., 2006b). Microneedle devices were therefore manufactured to investigate the capability of nanoparticles to permeate through a perforated human epidermal membrane. Pyramidal microneedles, with both pointed (Fig. 6A and B) and 'frustum' (Fig. 6C and D) shaped tips were created by wet-etch microfabrication techniques and employed as a means to create microdisruptions in the skin barrier (Wilke et al., 2005). Arrays were ~0.5 cm^2 and consisted of sixteen individual microneedles, approximately 280 μm in length and with base diameters of up to 200 μm (Fig. 6).

3.4. Propranolol diffusion through microneedle treated human epidermal membrane

The permeation of a low molecular weight drug through microneedle treated human epidermal membrane was initially assessed to confirm the penetrative capabilities of the manufactured microneedle devices. Propranolol, an easily analysed molecule examined previously in transdermal permeation studies (Modamio et al., 2000; Rama Rao et al., 2003; Stott et al., 2001), was selected as the model drug to validate the performance of microneedle devices. Recent published work from Prausnitz and colleagues has shown that a hydrochloride salt of naltrexone is delivered more efficiently through microneedle-treated skin when compared with unionised variants (Banks et al., 2008). The hydrochloride salt of propranolol was selected for this study.

Results indicate that less than 2% of a topically applied propranolol hydrochloride formulation was able to permeate through untreated human epidermal membrane (Fig. 7). However creation of microconduits by the microneedle device increased epidermal penetration to more than 15% of the applied dose (Fig. 7). This confirmed the functionality of the microneedle device, although significant standard deviation values indicated that the rate of permeation between diffusion cells was variable. Inconsistent penetration of the epidermal membrane would contribute to this variability, and may arise as a result of minor differences in thickness of the separated membrane or divergence in the number and/or dimensions of skin punctures on microneedle application. Some of these inconsistencies could potentially be overcome through using a more standardised microneedle application procedure.

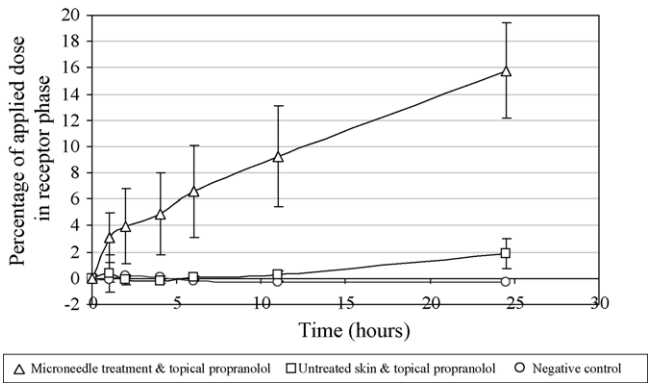

Fig. 7. Diffusion profiles detailing the percentage of the applied propranolol hydrochloride dose detected within the receptor phase of Franz-type diffusion cells. Diffusion of propranolol hydrochloride through untreated human epidermal membrane and human epidermal membranes treated with pointed microneedle devices was compared. Mean ± S.D. (N = 4 for untreated and microneedle treated membranes).

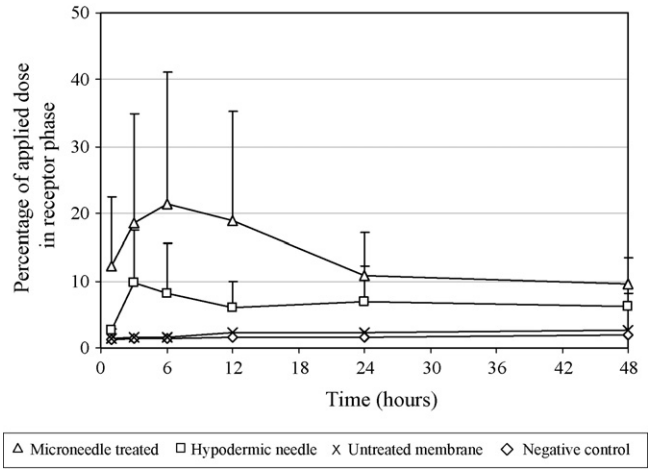

Fig. 8. Diffusion profiles detailing the percentage of the applied nanosphere formulation detected within the receptor phase of Franz-type diffusion cells over a period of 48 h. Diffusion of nanosphere formulations through untreated human epidermal membrane and human epidermal membranes treated with frustum tipped microneedle devices or a hypodermic needle (10 punctures) was compared. Mean ± S.D. ($N = 4$ for treated membranes).

3.5. Nanoparticle diffusion through microneedle treated human epidermal membrane

Few studies have investigated latex nanoparticle permeation through intact human skin tissue. Kohli et al (Kohli and Alpar, 2004) used porcine skin to investigate the permeation of nanoparticles across the untreated barrier and suggest that 50 and 500 nm negatively charged fluorescent latex nanoparticles can permeate across the SC and into the epidermal layer. However, in the same study, 200 and 300 nm nanoparticles failed to demonstrate such penetrative capabilities (Kohli and Alpar, 2004). In a more recent study, using confocal laser scanning microscopy to examine the penetration of topically applied negatively charged nanoparticles (20 and 200 nm in diameter) across porcine skin (Alvarez-Roman et al., 2004), investigators acknowledged that although particle size, surface charge and hydrophobicity affect nanoparticle penetration and deposition in a biological tissue, there was no evidence of penetration through intact SC.

Microneedle array devices have been investigated as a means to facilitate trans/intradermal delivery of macromolecular therapeutics (Birchall et al., 2005; Cormier et al., 2004; Coulman et al., 2006b; Gonzalez et al., 2008; Martanto et al., 2004; Mcallister et al., 1999, 2000, 2003; Roxhed et al., 2008; Smart and Subramanian, 2000). However nanoparticle permeation and distribution within microneedle treated skin is less well documented (Mcallister et al., 2003) and poorly characterised.

In this study, the permeation of 100 nm nanoparticles across untreated, microneedle treated and hypodermic needle treated human epidermal membrane was compared to investigate the penetrative enhancement induced by microneedle treatment of the skin. Negative controls served to determine minor 'background' levels of fluorescence in the receptor phase, most likely contributed by autofluorescent biological components leaching from the epidermal membrane into the receptor phase (equivalent to 2% of the applied dose at 48 h) (Fig. 8). Topical application of fluorescent nanospheres to untreated skin produced comparable levels of fluorescence to the negative control (2.6% of the applied dose at 48 h) (Fig. 8). Further to this, high-resolution SEM images of the untreated epidermal membrane, post-experimentation, illustrated the closely packed arrangement of corneocytes in the SC barrier (Fig. 9A) and permitted identification of individual nanospheres adhering to the skin surface and collecting within dermatoglyphics (Fig. 9B). These results support previous observations (Alvarez-Roman et al., 2004) and confirm the resistance of the outer epidermal barrier to passive diffusion of 100 nm negatively charged nanoparticles.

Perforation of the epidermal membrane by 10 punctures using a hypodermic needle created a number of uniform circular

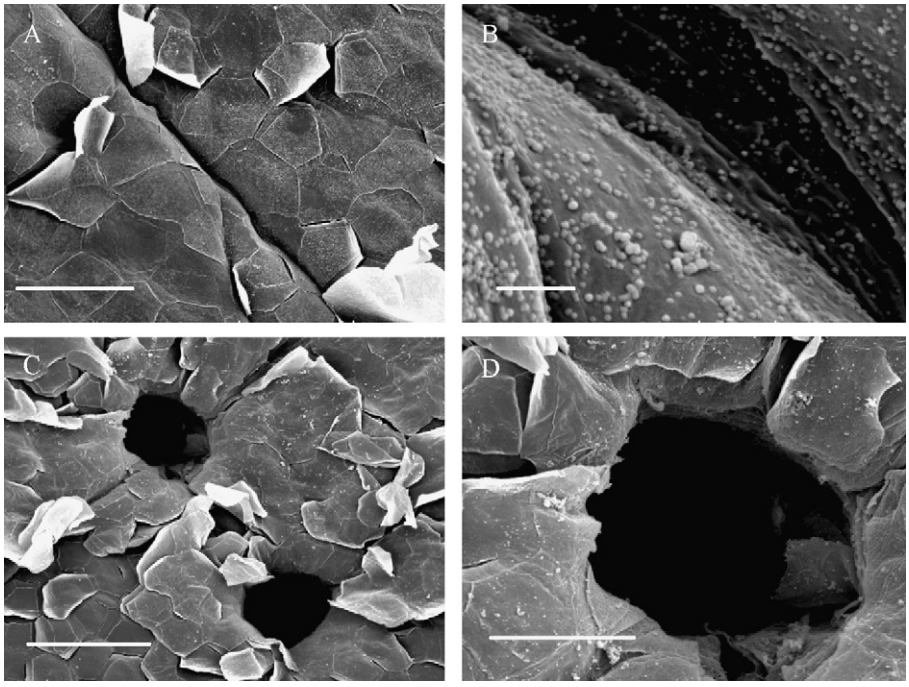

Fig. 9. Scanning electron micrographs of human epidermal membranes used in nanosphere diffusion experiments. Untreated epidermal membranes (A and B) and those treated with a hypodermic needle (C and D) following topical nanosphere application are pictured. (A and D) scale bar = 50 μm; (B) scale bar = 2 μm; (C) scale bar = 100 μm.

microchannels, 50–100 μm in diameter, in the skin surface (Fig. 9C and D). The compromised barrier permitted epidermal permeation of ~10% of the applied nanosphere formulation within 3 h of topical application (Fig. 8). However in a manner comparable to those studies conducted using model membranes (Section 3.2), receptor phase fluorescence decreased over the remaining time. In model studies the cessation in permeation and the subsequent reduction in fluorescence levels were attributed to electrostatic interaction of nanoparticles with the synthetic membrane surface, leading to progressive blockage of micropores, and interaction of those permeated nanoparticles with the underside of the membrane. This phenomenon may also influence nanoparticle permeation through the skin barrier although human epidermal membrane, a biological tissue, is considerably more complex and it is therefore more difficult to rationalise the data. However, physicochemical factors, including size exclusion and electrostatic interaction with one or more of the skin components, will contribute to the nanoparticle permeation through the treated epidermal membrane.

The application of frustum tipped microneedles to the skin surface resulted in more than 20% of the applied nanosphere formulation traversing the epidermal barrier over a 6 h period (Fig. 8). However in a manner synonymous to that observed with hypodermic needle treated tissue, permeation appeared to halt and fluorescence levels in the receptor phase subsequently diminished during the remainder of the experimental time (Fig. 8). SEM images of epidermal membranes used in diffusive studies indicate that microneedle induced micro-disruptions were of comparable diameter to those created by the hypodermic needle but were greater in number (Fig. 10). These preliminary studies suggest that a greater population of microchannels may enhance nanoparticle permeation through the treated tissue, although more extensive investigations with greater sample numbers are required in order to confirm this observation (Fig. 8). The most notable feature of microneedle permeation data was the recurrence of significant standard deviations associated with the data points (Fig. 8). This may be explained by inconsistencies in the quantity and geometry of microchannels both between and within samples. Microchannels created by the device were visualised as simple circular conduits (Fig. 10D) and also less symmetrical microdisruptions displaying lateral 'tares' in the membrane (Fig. 10A).

Closer inspection of the skin surface revealed the multi-layered organisation of corneocytes surrounding microchannels and, interestingly, the presence of surface adsorbed nanospheres between the disrupted corneocytes (Fig. 10E and F). Nanoparticles were also visible on the interior surface of microchannels (Fig. 10A, C and F) and in associated lateral disruptions (Fig. 10A and B). Interaction of the formulation with the viable epidermal tissue in this

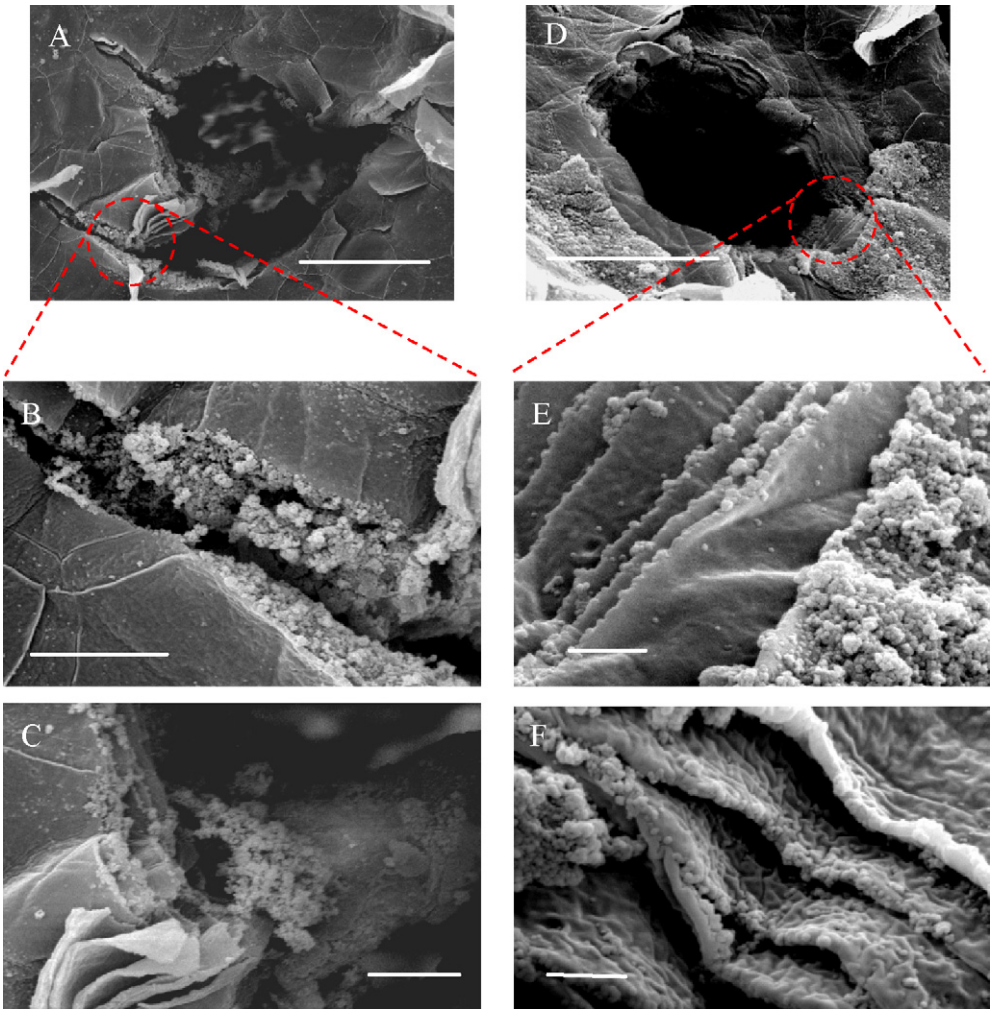

Fig. 10. Scanning electron micrographs of those human epidermal membranes treated with a frustum tipped wet-etch microneedle device following topical application of a fluorescent nanosphere formulation in diffusion experiments. (A and D) scale bar = 50 μm; (B and C) scale bar = 10 μm; (E and F) scale bar = 2 μm.

manner may retard transdermal delivery for systemic therapeutic application. However for therapeutic applications that required intradermal localisation, interaction of the formulation with the cells of the viable epidermis may prove beneficial, e.g. cutaneous gene delivery and vaccination. The monodisperse nanoparticle formulation remained stable in those studies using untreated epidermal membranes (Fig. 9). However, microneedle treatment of the skin appeared to stimulate aggregation of nanoparticles (Fig. 10B, C and F). Exposure of the underlying epidermal cells and/or the release of cellular components into the extracellular milieu may have contributed to destabilisation of the colloidal formulation. A combination of nanoparticle adherence to the tissue surface and aggregation of the colloidal system may therefore explain the progressive retardation and finally obstruction to effective transepidermal permeation (Fig. 8).

4. Conclusions

The model system described in these studies has demonstrated the significant impact of surface charge and pore size on the permeation characteristics of a nanoparticle formulation through microchannels, such as those created in microneedle treated skin. Results support the intuitive principle that maximising the diameter of those conduits that are created in the skin surface will facilitate more rapid and complete nanoparticle permeation. However the maximum dimensions of those conduits created in the skin for drug delivery purposes will also be governed by the desire for limited invasiveness from a pain and safety perspective. Electrostatic interaction of the nanoparticle formulation with the membrane or microchannel surface can also influence permeation characteristics and therefore surface charge of particles within a colloidal formulation must be carefully controlled to optimise delivery. Although the microneedle device has demonstrated aptitude in the localised delivery of a nanoparticle formulation across the human epidermal barrier, results showed a significant level of variability. High-resolution SEM images illustrated some of the complexities that are associated with microneedle mediated delivery of a nanoparticle formulation across a multi-layered tissue structure. Inconsistencies in microneedle penetration of the skin (i.e. not all microneedles on a single array piercing the skin upon each application and a difference in the structural characteristics of the created microconduits), the unpredictable stability of the colloidal formulation in the extracellular milieu and direct interaction of nanoparticles with the exposed tissue were identified as key determinants of nanoparticle permeation in this investigation.

These studies have demonstrated microneedle functionality for the trans/intradermal delivery of nanoparticle formulations. However, further work is required to characterise the physicochemical and biological barriers that influence both the permeation properties and, importantly for cutaneous delivery, the distribution of nanoparticle therapeutics within the skin strata. The development of a reliable and effective non-invasive delivery system for therapeutic applications such as cutaneous vaccination should therefore ensure synchronous development of the delivery platform, i.e. the microneedle device, and also the pharmaceutical formulation.

Acknowledgements

The authors would like to acknowledge the financial support of the RPSGB and the National Access Programme, TNI, Cork, Ireland. The authors also acknowledge the technical assistance of Dr. Antoine Hann in scanning electron microscopy studies.

References

Alvarez-Roman, R., Naik, A., Kalia, Y.N., Guy, R.H., Fessi, H., 2004. Skin penetration and distribution of polymeric nanoparticles. J. Control. Release 99, 53–62.
Apel, P., 2001. Track etching technique in membrane technology (invited talk). Radiat. Meas. 34, 559–566.
Banks, S.L., Pinninti, R.R., Gill, H.S., Crooks, P.A., Prausnitz, M.R., Stinchcomb, A.L., 2008. Flux across of microneedle-treated skin is increased by increasing charge of Naltrexone and Naltrexol in vitro. Pharm. Res. 25, 1677–1685.
Baroli, B., Ennas, M.G., Loffredo, F., Isola, M., Pinna, R., Lopez-Quintela, M.A., 2007. Penetration of metallic nanoparticles in human full-thickness skin. J. Invest. Dermatol. 127, 1701–1712.
Barry, B.W., 2001. Review: novel mechanisms and devices to enable successful transdermal drug delivery. Eur. J. Pharm. Sci. 14, 101–114.
Barry, B.W., 2002. Drug delivery routes in skin: a novel approach. Adv. Drug Del. Rev. 54, S31–S40.
Barry, M.E., Pinto-Gonzalez, D., Orson, F.M., Mckenzie, G.J., Petry, G.R., Barry, M.A., 1999. Role of endogenous endonucleases and tissue site in transfection and CpG-mediated immune activation after naked DNA injection. Hum. Gene Ther. 10, 2461–2480.
Birchall, J.C., Coulman, S., Pearton, M., Allender, C., Brain, K., Anstey, A., Gateley, C., Wilke, N., Morrissey, A., 2005. Cutaneous DNA delivery and gene expression in *ex vivo* human skin explants via wet-etch microfabricated microneedles. J. Drug Target 13, 415–421.
Bos, J.D., Meinardi, M.M.H.M., 2000. The 500 Dalton rule for the skin penetration of chemical compounds and drugs. Exp. Dermatol. 9, 165–169.
Brendler, E., Ratkje, S.K., Hertz, H.G., 1995. Streaming potentials of nuclepore membranes by the electric wok method. Electrochim. Acta 41, 169169–169176.
Burnette, R.R., Ongpipattanakul, B., 1987. Characterization of the permselective properties of excised human skin during iontophoresis. J. Pharm. Sci. 76, 765–773.
Campbell, R.B., 2006. Tumor physiology and delivery of nanopharmaceuticals. Anti Cancer Agents Med. Chem. 6, 503–512.
Chiarello, K., 2004. Breaking the barrier: advances in transdermal technology. Pharm. Technol. 28, 46–56.
Christophers, E., Kligman, A., 1963. Preparation of isolated sheets of human stratum corneum. Arch. Dermatol. 88, 702–704.
Combadiere, B., Mahe, B., 2008. Particle-based vaccines for transcutaneous vaccination. Comp. Immunol. Microbiol. Infect. Dis. 31, 293–315.
Cormier, M., Johnson, B., Ameri, M., Nyam, K., Libiran, L., Zhang, D.D., Daddona, P., 2004. Transdermal delivery of desmopressin using a coated microneedle array patch system. J. Control. Release 97, 503–511.
Coulman, S.A., Allender, C., Birchall, J.C., 2006a. Microneedles and other physical methods for overcoming the stratum corneum barrier for cutaneous gene therapy. Crit. Rev. Ther. Drug Carrier Syst. 23, 205–258.
Coulman, S.A., Barrow, D., Anstey, A., Gateley, C., Morrissey, A., Wilke, N., Allender, C., Brain, K., Birchall, J.C., 2006b. Minimally invasive cutaneous delivery of macromolecules and plasmid DNA via microneedles. Curr. Drug Deliv. 3, 65–75.
Cross, S.E., Roberts, M.S., 2004. Physical enhancement of transdermal drug application: is delivery technology keeping up with pharmaceutical development. Curr. Drug Deliv. 1, 81–92.
Diez, L.M., Villa, F.M., Giminez, A.H., Garcia, F.T., 1989. Streaming potential of some polycarbonate microporous membranes when bathed by LiCl, NaCl, $MgCl_2$ and $CaCl_2$ aqueous solutions. J. Colloid Interf. Sci. 132, 27–33.
Elias, P.M., 1983. Epidermal lipids, barrier function, and desquamation. J. Invest. Dermatol. 80, 44s–49s.
Elias, P.M., 2005. Stratum corneum defensive functions: an integrated view. J. Invest. Dermatol. 125, 183–200.
Florence, A.T., 2007. Pharmaceutical nanotechnology: more than size: ten topics for research. Int. J. Pharm. 339, 1–2.
Frerichs, D.M., Ellingsworth, L.R., Frech, S.A., Flyer, D.C., Villar, C.P., Yu, J.M., Glenn, G.M., 2008. Controlled, single-step, stratum corneum disruption as a pretreatment for immunization via a patch. Vaccine 26, 2782–2787.
Gadiraju, P.D., Park, J.H., Lee, J.W., Prausnitz, M.R., Allen, M.G., 2007. Micro-ablation of skin by arc-discharge jet ejection for transdermal drug delivery. In: Transducers '07 & Eurosensors, vol. XXI, pp. U982–U983.
Giudice, E.L., Campbell, J.D., 2006. Needle-free vaccine delivery. Adv. Drug Deliv. Rev. 58, 68–89.
Glenn, G.M., Kenney, R.T., 2006. Mass vaccination: solutions in the skin. In: Plotkin, S.A. (Ed.), Mass Vaccination: Global Aspects—Progress and Obstacles. Springer, New York, pp. 247–268.
Gonzalez, E.G., Speaker, T.J., Leake, D., Contag, C.H., Kaspar, R.L., 2008. In vivo delivery of functional macromolecules including siRNAs to skin by novel soluble-tip microneedle arrays. J. Invest. Dermatol. 128, S130–S1130.
Haq, M.I., Smith, E., John, D.N., Kalavala, M., Edwards, C., Anstey, A., Morrissey, A., Birchall, J.C., 2008. Clinical administration of microneedles: skin puncture, pain and sensation. Biomed. Microdevices [Epub ahead of print].
Henry, S., Mcallister, D.V., Allen, M., Prausnitz, M.R., 1998. Microfabricated microneedles: a novel approach to transdermal drug delivery. J. Pharm. Sci. 87, 922–925.
Hirschberg, H., De Wijdeven, G., Kelder, A.B., Van Den Dobbelsteen, G., Kerstena, G.F.A., 2008. Bioneedles (TM) as vaccine carriers. Vaccine 26, 2389–2397.
Hoet, P., Bruske-Hohlfeld, I., Salata, O., 2004. Nanoparticles—known and unknown health risks. J. Nanobiotechnol. 2, 12.

Huismann, I.H., Pradanos, P., Calvo, J.I., Hernandez, A., 2000. Electroviscous effects, streaming potential and zeta potential in polycarbonate track-etched membranes. J. Membr. Sci. 178, 79–92.
Keesom, W.H., Zelenka, R.L., Radke, C.J., 1988. A zeta-potential model for ionic surfactant adsorption on an ionogenic hydrophobic surface. J. Colloid Interf. Sci. 125, 575–585.
Kenney, R.T., Frech, S.A., Muenz, L.R., Villar, C.P., Glenn, G.M., 2004. Dose sparing with intradermal injection of influenza vaccine. N. Engl. J. Med. 351, 2295–2301.
Kohli, A.K., Alpar, H.O., 2004. Potential use of nanoparticles for transcutaneous vaccine delivery: effect of particle size and charge. Int. J. Pharm. 275, 13–17.
Kuntsche, J., Bunjes, H., Fahr, A., Pappinen, S., Rönkkö, S., Suhonen, M., Urtti, A., 2008. Interaction of lipid nanoparticles with human epidermis and an organotypic cell culture model. Int. J. Pharm. 354, 180–195.
La Montagne, J.R., Fauci, A.S., 2004. Effect of intradermal influenza vaccination—can less be more? N. Engl. J. Med. 351, 2330–2332.
Lademann, J., Weigmann, H.J., Rickmeyer, C., Barthelmes, H., Schaefer, H., Mueller, G., Sterry, W., 1999. Penetration of titanium dioxide microparticles in a sunscreen formulation into the Horny Layer and the follicular orifice. Skin Pharmacol. Physiol. 12, 247–256.
Lademann, J., Richter, H., Teichmann, A., Otberg, N., Blume-Peytavi, U., Luengo, J., Weiss, B., Schaefer, U.F., Lehr, C.M., Wepf, R., Sterry, W., 2007. Nanoparticles—an efficient carrier for drug delivery into the hair follicles. Eur. J. Pharm. Biopharm. 66, 159–164.
Lawson, L.B., Freytag, L.C., Clements, J.D., 2007. Use of nanocarriers for transdermal vaccine delivery. Clin. Pharmacol. Ther. 82, 641–643.
Lee, P.W., Peng, S.F., Su, C.J., Mi, F.L., Chen, H.L., Wei, M.C., Lin, H.J., Sung, H.W., 2008. The use of biodegradable polymeric nanoparticles in combination with a low-pressure gene gun for transdermal DNA delivery. Biomaterials 29, 742–751.
Liu, Y., Costigan, G., Bellhouse, B.J., 2008. Performance studies of a conical nozzle designed for the macromolecular skin delivery. J. Drug. Target 16, 206–212.
Manolova, V., Flace, A., Bauer, M., Schwarz, K., Saudan, P., Bachmann, M.F., 2008. Nanoparticles target distinct dendritic cell populations according to their size. Eur. J. Immunol. 38, 1404–1413.
Martanto, W., Davis, S.P., Holiday, N.R., Wang, J., Gill, H.S., Prausnitz, M.R., 2004. Transdermal delivery of insulin using microneedles *in vivo*. Pharm. Res. 21, 947–952.
Mcallister, D.V., Kaushik, S., Patel, P.N., Mayberry, J.L., Allen, M.G., Prausnitz, M.R.D.V.M. (Eds.), 1999. Proc. Int. Symp. Control Release. Bioact. Mater., vol. 26. Controlled Release Society, Boston, pp. 192–193.
Mcallister, D.V., Allen, M.G., Prausnitz, M.R., 2000. Microfabricated microneedles for gene and drug delivery. Annu. Rev. Biomed. Eng. 2, 289–313.
Mcallister, D.V., Wang, P.M., Davis, S.P., Park, J.H., Canatella, P.J., Allen, M.G., Prausnitz, M.R., 2003. Microfabricated Needles for Transdermal Delivery of Macromolecules and Nanoparticles: Fabrication Methods and Transport Studies, 100. PNAS, USA, pp. 13755–13760.
Mikszta, J.A., Alarcon, J.B., Brittingham, J.M., Sutter, D.E., Pettis, R.J., Harvey, N.G., 2002. Improved genetic immunization via micromechanical disruption of skin-barrier function and targeted epidermal delivery. Nat. Med. 8, 415–419.
Mikszta, J.A., Sullivan, V.J., Dean, C., Waterston, A.M., Alarcon, J.B., Dekker, J.P., Brittingham, J.M., Huang, J., Hwang, C.R., Ferriter, M., Jiang, G., Mar, K., Saikh, K.U., Stiles, B.G., Roy, C.J., Ulrich, R.G., Harvey, N.G., 2005. Protective immunization against inhalational anthrax: a comparison of minimally invasive delivery platforms. J. Infect. Dis. 191, 278–288.
Mitragotri, S., 2004. Breaking the skin barrier. Adv. Drug Deliv. Rev. 56, 555–556.
Modamio, P., Lastra, C.F., Marino, E.L., 2000. A comparative *in vitro* study of percutaneous penetration of [beta]-blockers in human skin. Int. J. Pharm. 194, 249–259.
Nasseri, B., Florence, A.T., 2005. The relative flow of the walls of phospholipid tether bilayers. Int. J. Pharm. 298, 372–377.
Papazoglou, E.S., Babu, S., Fan, C., Sunkari, C., Uitto, J., 2008. Particle size and bilayer rigidity effects on skin diffusion of nanosomes. J. Invest. Dermatol. 128, S54.
Pearton, M., Allender, C., Brain, K., Anstey, A., Gateley, C., Wilke, N., Morrissey, A., Birchall, J., 2008. Gene delivery to the epidermal cells of human skin explants using microfabricated microneedles and hydrogel formulations. Pharm. Res. 25, 407–416.
Prausnitz, M.R., 2004. Microneedles for transdermal drug delivery. Adv. Drug Deliv. Rev. 56, 581–587.
Prausnitz, M.R., Mitragotri, S., Langer, R., 2004. Current status and future potential of transdermal drug delivery. Nat. Rev. Drug Discov. 3, 115–124.
Rama Rao, P., Reddy, M.N., Ramakrishna, S., Diwan, P.V., 2003. Comparative in vivo evaluation of propranolol hydrochloride after oral and transdermal administration in rabbits. Eur. J. Pharm. Biopharm. 56, 81–85.
Roxhed, N., Samel, B., Nordquist, L., Griss, P., Stemme, G., 2008. Painless drug delivery through microneedle-based transdermal patches featuring active infusion. IEEE Trans. Biomed. Eng. 55, 1063–1071.
Ruenraroengsak, P., Florence, A.T., 2005. The diffusion of latex nanospheres and the effective (microscopic) viscosity of HPMC gels. Int. J. Pharm. 298, 361–366.
Ruponen, M., Honkakoski, P., Ronkko, S., Pelkonen, J., Tammi, M., Urtti, A., 2003. Extracellular and intracellular barriers in non-viral gene delivery. J. Control. Release 93, 213–217.
Salata, O.V., 2004. Applications of nanoparticles in biology and medicine. J. Nanobiotechnol. 2, 3.
Sanna, V., Gavini, E., Cossu, M., Rassu, G., Giunchedi, P., 2007. Solid lipid nanoparticles (SLN) as carriers for the topical delivery of econazole nitrate: in-vitro characterization, ex-vivo and in-vivo studies. J. Pharm. Pharmacol. 8, 1057–1064.
Scheulplein, R.L., Blank, I.H., 1971. Permeability of the skin. Physiol. Rev. 51, 702–747.
Schuetz, Y.B., Naik, A., Guy, R.H., Kalia, Y.N., 2005. Emerging strategies for the transdermal delivery of peptide and protein drugs. Expert Opin. Drug Deliv. 2, 533–548.
Sheiheta, L., Chandra, P., Batheja, P., Devore, D., Kohn, J., Michniak, B., 2008. Tyrosine-derived nanospheres for enhanced topical skin penetration. Int. J. Pharm. 350, 312–319.
Smart, W.H., Subramanian, K., 2000. The use of silicon microfabrication technology in painless blood glucose monitoring. Diabetes Technol. Ther. 2, 549–559.
Stott, P.W., Williams, A.C., Barry, B.W., 2001. Mechanistic study into the enhanced transdermal permeation of a model [beta]-blocker, propranolol, by fatty acids: a melting point depression effect. Int. J. Pharm. 219, 161–176.
Sugrue, S., 1992. Predicting and controlling colloid suspension stability using electrophoretic mobility and particle size measurements. Am. Lab. 24, 64–71.
Ting, W.W., Vest, C.D., Sontheimer, R.D., 2004. Review of traditional and novel modalities that enhance the permeability of local therapeutics across the stratum corneum. Int. J. Dermatol. 43, 538–547.
Toll, R., Jacobi, U., Richter, H., Lademann, J., Schaefer, H., Blume-Peytavi, U., 2003. Penetration profile of microspheres in follicular targeting of terminal hair follicles. J. Invest. Dermatol. 123, 168–176.
Wertz, P.W., Van Den Bergh, 1998. Review. The physical, chemical and functional properties of lipids in the skin and other biological barriers. Chem. Phys. Lipids 91, 85–96.
Widera, G., Johnson, J., Kim, L., Libiran, L., Nyam, K., Daddona, P.E., Cormier, M., 2006. Effect of delivery parameters on immunization to ovalbumin following intracutaneous administration by a coated microneedle array patch system. Vaccine 24, 1653–1664.
Wilke, N., Mulcahy, A., Ye, S.-R., Morrissey, A., 2005. Process optimization and characterization of silicon microneedles fabricated by wet etch technology. Microelectron. J. 36, 650–656.
Zhang, L.W., Monteiro-Riviere, N.A., 2008. Assessment of quantum dot penetration into intact, tape-stripped. Abraded and flexed rat skin. Skin Pharmacol. Physiol. 21, 166–180.
Zhang, L.W., Yu, W.W., Colvin, V.L., Monteiro-Riviere, N.A., 2008. Biological interactions of quantum dot nanoparticles in skin and in human epidermal keratinocytes. Toxicol. Appl. Pharmacol. 228, 200–211.